**RESEARCH ARTICLE**

CrossMark

# Phosphate affects adsorption and desorption of oxytetracycline in the seawater-sediment systems

Jia Li[1,2] · Hua Zhang[2] · Guodong Yuan[3]

## Abstract

The fate and transport of antibiotics in the aquatic environment are usually influenced by the combined effects of environmental factors. In this study, batch-type experiments were conducted to investigate the combined effects of phosphate and salinity on oxytetracycline (OTC) adsorption on, and desorption from, two marine sediments. Pseudo-second-order kinetic model fitted the kinetic data better than pseudo-first-order model. The pseudo-second-order kinetic rate ($k_2$) of OTC increased significantly with increasing phosphate concentrations. Sorption isotherms of OTC can be well described by both the Langmuir and Freundlich models. Compared with the control experiments (without phosphate addition), Freundlich distribution coefficients ($K_F$) after addition of 50 mg L$^{-1}$ phosphate decreased from 24.9 to 17.9 L kg$^{-1}$ on sediments collected from Laizhou Bay, and from 52.2 to 31.3 L kg$^{-1}$ on sediments collected from Bohai Bay, which indicated that phosphate could inhibit adsorption of OTC on marine sediments. Furthermore, phosphate had a stronger inhibitory effect on OTC adsorption at low salinity level than at high salinity level. The effects of phosphate on OTC adsorption can be explained by ion exchange, change of sediment surface charge, and electrostatic repulsion mechanisms. Desorption experiments showed that phosphate can enhance the total desorption percentage of OTC from marine sediments. Overall, the presence of phosphate in marine system may enhance OTC's long-term transport.

**Keywords** Oxytetracycline · Phosphate · Sorption/desorption · Salinity · Combined effects · Kinetics

## Introduction

Oxytetracycline (OTC) has been widely used for humans and animals. In China alone, more than 1300 tons of OTC was consumed in 2013 (Zhang et al. 2015). A huge percentage of consumed OTC was excreted in unchanged or active forms

✉ Hua Zhang
  hzhang@yic.ac.cn

1 School of Environmental Science and Engineering, Yangzhou University, Yangzhou 225127, People's Republic of China

2 Key Laboratory of Coastal Environmental Process and Ecology Remediation, Yantai Institute of Coastal Zone Research, Chinese Academy of Sciences, Yantai 264003, People's Republic of China

3 School of Environmental and Chemical Engineering, Zhaoqing University, Zhaoqing 526061, People's Republic of China

(Hirsch et al. 1999) and then discharged into the recipient environments, which could increase bacterial resistance and contribute to the emerging of antibiotics resistance genes (Zhang and Zhang 2011). Resistant bacteria can persist in aquatic environment for 5 or 10 years (Nonaka et al. 2007), and OTC-resistant bacteria in marine sediment and seawater have increased over time (Gao et al. 2012).

Adsorption-desorption process is a key determinant of the fate and transport of antibiotics at sediment/water interface. The main adsorption mechanisms of OTC include ion exchange, electrostatic attraction, hydrophobic interaction, and surface complexation (Jones et al. 2005). Both adsorbent and environmental factors have great impacts on these processes (ter Laak et al. 2006; Carrasquillo et al. 2008; Song et al. 2014). Competing anions, pH, and ionic strength, for example, can change the electric charge characteristics of sediments and OTC, thus influencing their interactions.

Among competing anions for OTC adsorption onto sediment, phosphate is of importance (Liu et al. 2012). While being an essential nutrient for organisms, phosphate in excess of needs could cause eutrophication (Li et al. 2013). In coastal/estuary ecosystems, sediment is the dominant phosphate

reservoir (Lebo 1991; Zwolsman 1994) because of the strong affinities of metal hydroxides in sediment for phosphate (Arai and Sparks 2007; Wang and Li 2010). Phosphate, however, would compete for adsorption sites onto sediment with other compounds, such as phthalic acid, salicylic acid, and 2,4-dichlorophenoxyacetic acid (2,4-D) (Vasudevan and Cooper 2004; Xu et al. 2007).

With phenolic hydroxyl, carbonyl, and amino groups, OTC is an amphoteric molecule. Its acid dissociation constants are $pK_{a1} = 3.27$, $pK_{a2} = 7.3$, and $pK_{a3} = 9.11$ (Florence and Attwood 2015). As OTC is negatively charged in marine environment (pH around 8), its adsorption-desorption behavior and its fate and transport in seawater-sediment system would be affected by phosphate. The competition of phosphate for tetracycline adsorption on Fe-Mn binary oxide (Liu et al. 2012) and soils (Wang et al. 2010a, b) has been investigated in freshwater or single electrolyte solution, which is less complex than marine environment where high ionic strength (salinity) affects the surface charge characteristics of sediments. To our knowledge, there is scarce data that elucidate the mechanisms of phosphate and OTC adsorption-desorption or their competitive adsorption behaviors in seawater-sediment systems. Further, the impacts of phosphate on OTC adsorption at different salinity remain unknown. Although pH has great impacts on reaction of antibiotics and phosphate (Wang et al. 2010a, b), it is not chosen as a factor in our study because pH is relatively stable in coastal seawater. On the contrary, salinity varies from 0 to 36‰ in estuary/coastal regions (Zhang and Huang 2011).

This study aimed to improve the understanding of combined effects of environmental factors on adsorption-desorption of OTC in the seawater-sediment system. To this end, experiments were conducted (a) to investigate adsorption kinetics of OTC as affected by phosphate, (b) to investigate the effect of phosphate on adsorption and desorption of OTC in the seawater-sediment system with equilibrium batch experiments, (c) to evaluate the combined effects of phosphate and salinity on OTC adsorption processes, and (d) to reveal the possible bonding mechanisms between OTC and marine sediment using FTIR analysis.

## Materials and methods

### Chemicals and marine sediment samples

Pure oxytetracycline was purchased from Sigma (USA). Other reagents and solvents were of analytical grade or better. Ultrapure water (MQ) was obtained from a Milli-Q water purification system (Millipore, Billerica, MA, USA). OTC was dissolved in methanol to prepare stock solution from which working solutions were prepared by diluting it with seawater collected from Bohai Sea. Before use, seawater was filtered through 0.22-μm membranes (JinTeng, China) and irradiated with ultraviolet light for 12 h to eliminate the influences of dissolved organic matter as much as possible. The pH of seawater is measured using a potentiometric titration (Metrohm, Switzerland) and the value is 8.0. The salinity of seawater is measured using a salinometer (ATAGO, Japan) and the value is 30‰. Phosphate concentration of seawater is measured using a Continuous Flow Auto Analyzer III (Seal, Germany) and the background concentration of phosphate is 20.4 μg L$^{-1}$.

Two surface marine sediment samples were collected from Bohai Bay (BHB) and Laizhou Bay (LZB). The sediment samples were placed into a freeze dryer (Songyuan, China) for 4 days to remove all the water. The detail information of marine sediment samples was described previously (Li and Zhang 2016). Briefly, the point of zero charge (PZC) was 9.2 for sediment BHB, and 9.4 for sediment LZB, suggesting a small amount of net positive charge during adsorption/desorption experiments (pH = 7.7~8.0); the total organic carbon contents in sediment BHB and LZB were 0.48% and 0.15%, respectively; the clay fraction (< 4 μm) in sediment BHB and LZB were 30.7% and 8.5%, respectively. Iron (Fe) oxide and aluminum (Al) oxide contents of marine sediments were analyzed using the methods described by Jones et al. (2005). The free Fe and Al oxides were extracted with sodium citrate-dithionite-bicarbonate at 80 °C and the non-crystalline Al and Fe oxides were extracted with acidified ammonium oxalate in the dark. Fe and Al elements were detected using inductively coupled plasma optical emission spectrometer (Optima 7000 DV, USA). The contents of Al and Fe oxides were shown in Table S1.

## Adsorption and desorption experiments

### Kinetic adsorption experiments

Kinetic adsorption experiments were carried out at 25 °C, by adding 10 mL OTC solution of 4 mg L$^{-1}$ into 30-mL glass vials with 0.2 g dry sediment. The suspensions contained either 10 or 50 mg P L$^{-1}$ to allow the assessment of phosphate effect on OTC adsorption rate. The glass vials were shaken in a temperature-controlled shaking incubator (Harbin, China) at a shaking speed of 190 rpm. The shaking incubator was covered with black cloth to prevent photo-degradation. The glass vials were taken out at 0.5, 1, 1.5, 2, 4, 6, 8, 12, 24, and 32 h, and centrifuged at 4000 rpm for 10 min. The obtained supernatants were filtered through a 0.22-μm syringe filter before analysis.

### Single solute adsorption experiments

To initiate the single solute adsorption experiments, 0.2 g of dry sediments were added into 30-mL glass vials, followed by

adding treated seawater with sodium azide of 0.2% (by weight). OTC standard solution was then added to make up the suspension volume of 10 mL in each glass vial. Final concentrations of OTC in the mixture were 0.5, 1, 5, 10, and 15 mg L$^{-1}$. The glass vials were shaken in dark at 25 °C for 24 h in the shaking incubator. After equilibrium, sample treatment was similar to kinetic adsorption experiments. For the salinity study, experiments were conducted in the diluted seawater with salinity of 5‰, 13‰, and 30‰, and the experimental procedures were similar to the test of single OTC adsorption. Two blank adsorption experiments, one with the reactor system containing OTC without sediment and the other containing sediment without OTC, were carried out. All adsorption studies were conducted in triplicate. The experimental procedures of single phosphate adsorption were accordant with single OTC adsorption experiments.

### Double solute adsorption experiments

To investigate the impact of phosphate on OTC adsorption, the treated seawater with a defined amount of phosphate (5, 10, 50 mg P L$^{-1}$) was used as background solution. Effects of salinity on the competitive adsorption experiments were also assessed. All the procedures of the double solute sorption experiments were similar to the single OTC adsorption experiment.

### Desorption experiments

A series of glass vials with 0.2 g dry sediment and 10 mL OTC solution of 15 mg L$^{-1}$ were shaken at 25 °C in the shaking incubator. After 24 h, the vials were centrifuged and the supernatants were filtered through a 0.22-μm syringe filter for analysis. The residue in vials was freeze-dried for 12 h. Then, 10 mL of seawater or seawater with different concentrations (10 and 50 mg L$^{-1}$) of phosphate was added into the glass vials to conduct desorption experiments in triplicate, and the procedures were similar to adsorption tests. Desorption experiments were repeated until no OTC was detected.

### Measurements and data analyses

OTC in solution was detected using high-performance liquid chromatography (Exformma 1600, USA) equipped with a UV detector set at 268 nm, and a Waters SunFire C18 column (2.1 × 150 mm, 3.5 μm particles). The column temperature was 35 °C. The flow rate was 0.3 mL min$^{-1}$ and injection volume was 50 μL. Mobile phase A was acetonitrile and B was ultrapure water with 0.4% acetic acid (12:88, v/v). The quantification of phosphate was performed using the molybdate blue method on a Continuous Flow Auto Analyzer III (Seal, Germany).

The amounts of OTC or phosphate adsorbed on sediments were calculated using the following equation:

$$q = (C_0 - C_t) \times V/m \qquad (1)$$

where $q$ (mg g$^{-1}$) is the amounts absorbed, $C_0$ (mg L$^{-1}$) is the concentration in the control, $C_t$ (mg L$^{-1}$) is the concentration at different sampling time, $V$ (mL) is solution volume, and $m$ (mg) is sediment mass.

### Fourier transform infrared spectroscopy

Original marine sediment samples and sediments loaded with 15 mg L$^{-1}$ OTC were analyzed using Fourier transform infrared (FTIR) spectroscopy (FT/IR-4100, JASCO, Japan). Samples were obtained following the procedure used for the batch adsorption experiments at the highest concentration (15 mg L$^{-1}$) of OTC. After centrifugation, the residue was freeze-dried. The dried sample was mixed with pure potassium bromide and then ground in agate mortar. The mixture was then pressed to a pellet for analysis. A 16-cm$^{-1}$ resolution was applied in recording the spectra. A background spectrum of air was collected and subtracted from the spectra of each sample.

## Results and discussion

### Adsorption kinetics

Figure 1 shows the effects of different phosphate concentrations (0, 10, and 50 mg L$^{-1}$) on adsorption kinetics of OTC. Generally speaking, adsorption equilibrium was achieved within 24 h. Obviously, OTC adsorption was extremely rapid in the initial 4 h, accounting for 75% of total adsorption for sediment LZB and 74% for BHB. This may be due to the high concentration gradient in the beginning of adsorption, which exhibited a strong driving force for the transport of OTC from solution to the surface of sediments. OTC adsorption on both sediments decreased with increasing phosphate concentrations, which was consistent with equilibrium experiments.

In order to understand the kinetic behavior of OTC adsorption onto marine sediments, the experimental data were fitted into pseudo-first-order model (Eq. (2)) and pseudo-second-order model (Eq. (3)).

$$q_t = q_e\left(1 - e^{-k_1 t}\right) \qquad (2)$$

$$\frac{t}{q_t} = \frac{t}{q_e} + \frac{1}{k_2 q_e^2} \qquad (3)$$

where $q_t$ and $q_e$ (mg g$^{-1}$) are the amounts of OTC adsorbed at time $t$ (h) and at equilibrium, respectively, and $k_1$ (h$^{-1}$) and $k_2$ (g mg$^{-1}$ min$^{-1}$) are rate constants for pseudo-first order and pseudo-second order, respectively.

**Fig. 1** Adsorption kinetics of OTC as affected by phosphate with different concentrations on sediment LZB (left) and sediment BHB (right). Solid lines are pseudo-second-order kinetic model simulations; dash lines are pseudo-first-order kinetic model simulations
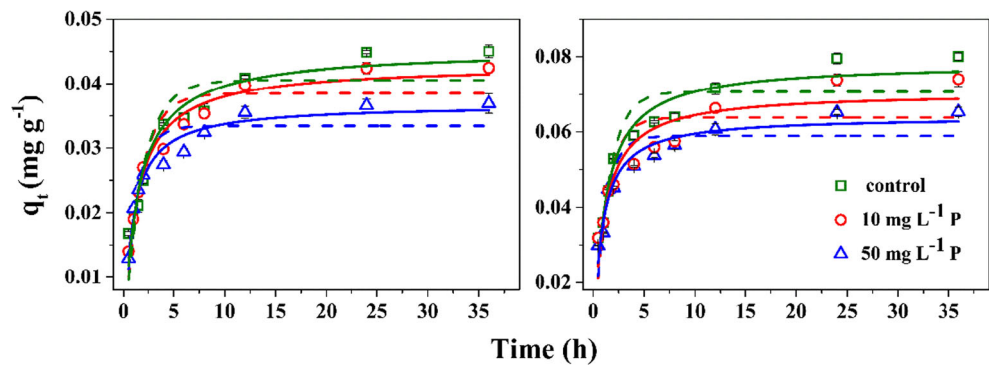


The kinetic model parameters were summarized in Table 1. The $R^2$ values were higher for pseudo-second-order model than pseudo-first-order model for both sediments. Furthermore, the adsorption capacity ($q_{e,cal}$) obtained from the pseudo-second-order kinetic model was closer to the experimental data ($q_{e,exp}$). Similar results were reported by Sun et al. (2012) for OTC adsorption on activated carbon. The pseudo-second-order kinetic rate ($k_2$) of OTC increased significantly with the increase of phosphate concentrations. As shown in Table 1, when phosphate concentration increased from 0 to 50 mg L$^{-1}$, $k_2$ increased from $15.6 \pm 2.87$ to $30.0 \pm 4.24$ g mg$^{-1}$ h$^{-1}$ for sediment LZB and from $11.9 \pm 2.06$ to $20.4 \pm 3.22$ g mg$^{-1}$ h$^{-1}$ for sediment BHB. This might be explained by (a) phosphate can be adsorbed preferentially and (b) a large number of phosphate anions occupied the active adsorption sites of sediments, which makes less adsorptive sites available for OTC to achieve equilibrium.

## Adsorption isotherms of single OTC and single phosphate on marine sediments

The adsorption isotherms of single OTC (no phosphate was added to the solution) and single phosphate (no OTC was added) on marine sediments are shown in Fig. 2. The adsorption isotherms were fitted into linear model $q = K_d C_e$ ($q$ is the mass of OTC sorbed per unit mass of sediment, $K_d$ is the partition coefficient, and $C_e$ is the equilibrium OTC concentration in the aqueous phase), Langmuir model $q = q_{max}$

$\frac{k_L C_e}{1 + k_L C_e}$ ($q_{max}$ is maximum sorption amount, $K_L$ (L mg$^{-1}$) is the Langmuir adsorption coefficient that can be related to binding strength), and Freundlich model $q = K_F C_e^n$ ($K_F$ is the Freundlich distribution coefficient and $n$ is a nonlinear coefficient). The best-fit parameters are summarized in Table S2. Overall, both Langmuir and Freundlich equations could fit adsorption data well, as demonstrated by their high $R^2$ values.

Sediment BHB showed higher OTC and phosphate adsorption capacities than LZB (Fig. 2). For example, the distribution coefficient $K_F$ for OTC adsorption on sediment BHB (52.2 L kg$^{-1}$) was higher than that for sediment LZB (24.9 L kg$^{-1}$). We ascribed these results to the higher contents of organic carbon (OC), clay, and metal oxides of sediment BHB because OTC and phosphate adsorption was highly correlated with Fe and Al contents (Figueroa and Mackay 2005; Zhang et al. 2009; Liu et al. 2012) and specific surface area in relation to clay and OC (Wang and Li 2010; Vasudevan and Cooper 2004). Marine sediments or montmorillonite with a higher clay content were reported having a higher adsorption capacity for tetracyclines (Xu and Li 2010). Barbooti (2017) demonstrated that adsorption of OTC on sediment is controlled mainly by the iron contents.

## Effect of phosphate on OTC adsorption

Figure 3 illustrates the effect of phosphate concentration on OTC adsorption on sediments. A significantly negative correlation ($p < 0.01$) was observed between them. Similar

**Table 1** Pseudo-first- and pseudo-second-order kinetic model parameters for adsorption of OTC on marine sediments

| Sediment | P mg L$^{-1}$ | $q_{(e,exp)}$ | Pseudo-first order model | | | Pseudo-second-order model | | |
|---|---|---|---|---|---|---|---|---|
| | | | $q_{(e,cal)}$ mg g$^{-1}$ | $k_1$ h$^{-1}$ | $R^2$ | $q_{(e,cal)}$ mg g$^{-1}$ | $k_2$ g mg$^{-1}$ h$^{-1}$ | $R^2$ |
| LZB | 0 | 0.0449 | 0.0405 | $0.540 \pm 0.100$ | 0.830 | 0.0452 | $15.6 \pm 2.87$ | 0.940 |
| | 10 | 0.0424 | 0.0385 | $0.600 \pm 0.0962$ | 0.870 | 0.0430 | $18.0 \pm 2.27$ | 0.971 |
| | 50 | 0.0366 | 0.0334 | $0.823 \pm 0.130$ | 0.848 | 0.0368 | $30.0 \pm 4.24$ | 0.957 |
| BHB | 0 | 0.0796 | 0.0707 | $0.707 \pm 0.128$ | 0.809 | 0.0783 | $11.9 \pm 2.06$ | 0.938 |
| | 10 | 0.0739 | 0.0638 | $0.797 \pm 0.180$ | 0.683 | 0.0706 | $14.9 \pm 3.55$ | 0.875 |
| | 50 | 0.0652 | 0.0589 | $0.914 \pm 0.154$ | 0.796 | 0.0641 | $20.4 \pm 3.22$ | 0.938 |

**Fig. 2** Adsorption isotherms of OTC or phosphate alone on sediments
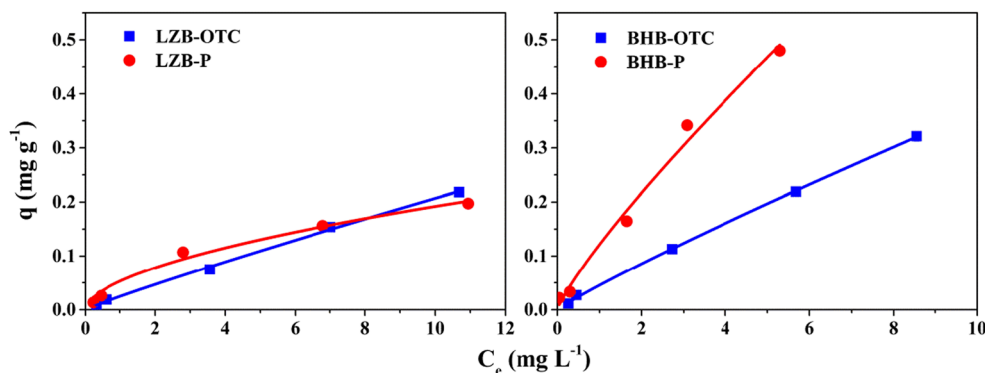


correlation was observed between tetracycline adsorption on soils and phosphate (Wang et al. 2010a, b). To further illustrate phosphate effects, Freundlich coefficient $K_F$ was plotted against phosphate concentration (Fig. 4). As phosphate increased from 0 to 50 mg L$^{-1}$, $K_F$ decreased from 24.9 to 17.9 L kg$^{-1}$ for LZB and from 52.2 to 31.3 L kg$^{-1}$ for BHB. Langmuir adsorption maxima $q_{max}$ showed a similar trend (Table S3).

As both phosphate and OTC can be adsorbed by marine sediments, they would compete for adsorption sites on the sediments. Though anionic OTC species combine with cations and iron oxide easier than zwitterionic species (Figueroa and Mackay 2005), phosphate formed even stronger ion pairs with divalent cations and stable inner-sphere complexes with metal oxides (Gao and Mucci 2003; Wang and Li 2010). Besides directly reducing OTC adsorption through competition, phosphate adsorption indirectly lowered OTC adsorption by creating more negative charge on marine

sediments (Vasudevan and Cooper 2004) and thus increasing electrostatic repulsion between anionic OTC and sediments.

## Effects of salinity on adsorption of OTC and phosphate

Salinity of seawater in estuary or coastal regions usually varied in a wide range due to the combined diluting effects of stream flow input and precipitation (Sumner and Belaineh 2005). Salinity, or ionic strength, altered the surface charge of sediments (Gao and Mucci 2003) and thus had a great impact on tetracycline and phosphate adsorption in a seawater-sediment system (Xu and Li 2010; Zhang and Huang 2011). To better understand adsorption behaviors of OTC and phosphate on marine sediments under different salinity levels, batch equilibrium experiments with salinity of 5‰, 13‰, and 30‰ were conducted.

**Fig. 3** Adsorption isotherms of OTC on sediment LZB (left) and sediment BHB (right). **a, b** Effect of phosphate with different concentrations on OTC adsorption (salinity = 30‰). **c, d** Combined effects of phosphate and salinity on OTC adsorption. Solid and dotted lines are Freundlich model simulations
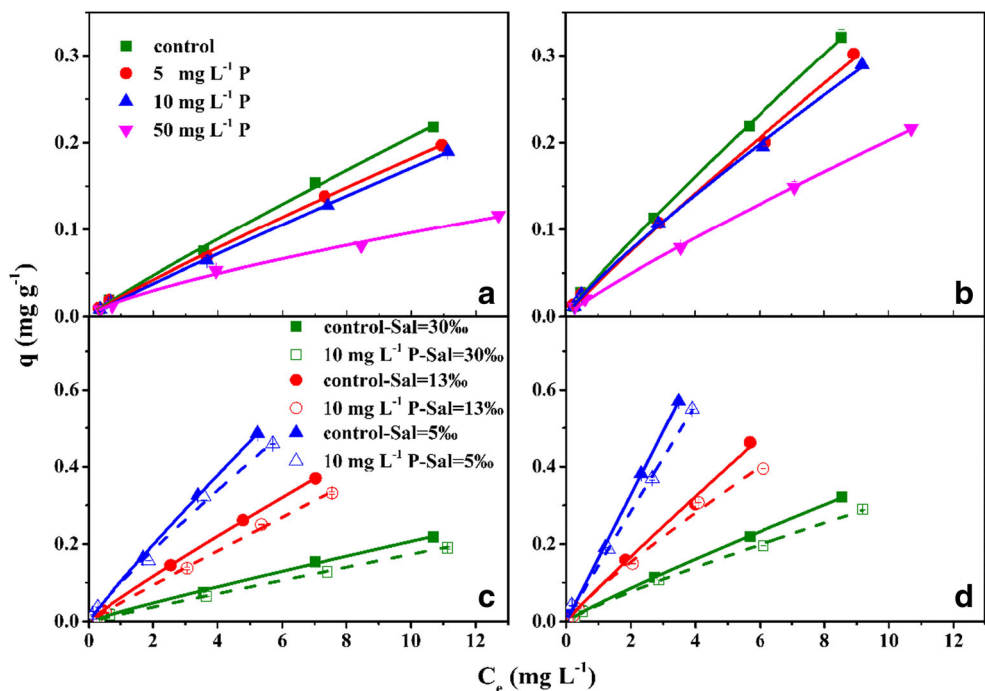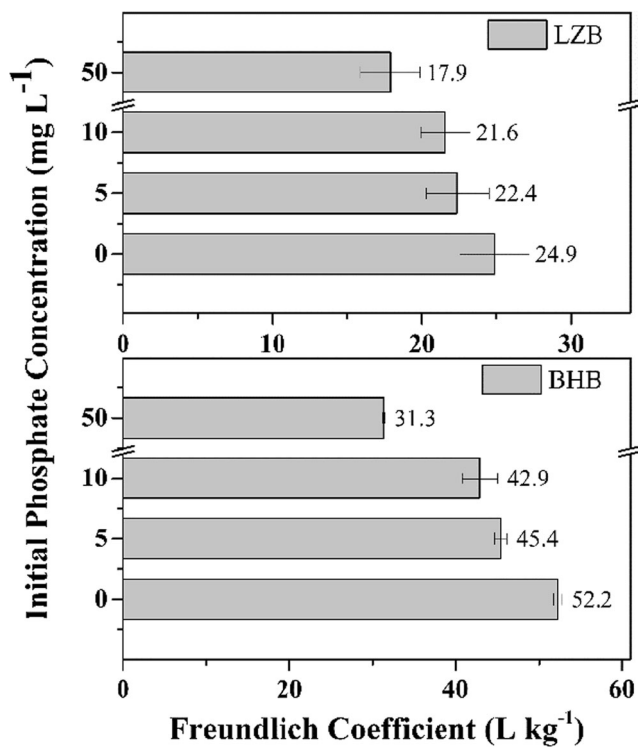
**Fig. 4** Freundlich distribution coefficient ($K_F$) values of OTC as affected by phosphate with different concentrations on sediment LZB and sediment BHB

As salinity increased, single OTC and single phosphate adsorption decreased on both LZB and BHB (Fig. 3 and Fig. S1). This is in consistent with earlier reports that low salinity promoted tetracycline and phosphate adsorption on marine sediments (Wang et al. 2010a, b; Zhang and Huang 2011). OTC adsorption maxima $q_{max}$ decreased significantly from 5.71 to 1.74 mg g$^{-1}$ for LZB and from 8.70 to 2.46 mg g$^{-1}$ for BHB as salinity increased from 5 to 30‰ (Table S4). Meanwhile, the Freundlich coefficient $K_F$ of phosphate reduced by 7.77% for LZB and by 20.3% for BHB. These reductions could be explained in three ways: (a) at high salinity level, abundant anions may compete for adsorption sites on sediments with deprotonated OTC species and phosphate, resulting in their reduced adsorption. For example, the presence of sulfate could suppress the adsorption of phosphate (Gao and Mucci 2003) and tetracycline (Liu et al. 2012); (b) abundant cations may also suppress adsorption of phosphate. Phosphate could form strong ion pairs with Ca$^{2+}$ and Mg$^{2+}$, enhance the electrostatic repulsion between the ion pairs, and positively charged marine sediments (PZC of 9.2 and 9.4) and thus decrease phosphate adsorption; and (c) hydrophobic interaction among anionic tetracycline molecules could overpower the electrostatic repulsion under high ionic strength condition to form aggregation of tetracycline molecules (Turku et al. 2007). Because OTC has a structure similar to tetracycline, we therefore hypothesized that OTC molecules formed aggregate under high ionic strengths and became more

difficult to reach the adsorption sites of sediments, resulting in a lower adsorption of OTC at high salinity level.

## Combined effects of phosphate and salinity on OTC adsorption

As demonstrated above, the presence of phosphate or a change in seawater salinity had a separate effect on OTC adsorption on marine sediments. However, in the estuarine/coastal waters, changes in seawater salinity and phosphate are probably to occur simultaneously. Their combined effects on OTC adsorption are shown in Figs. 3c and 2d. Phosphate anion reduced OTC adsorption at three different salinity levels. To further explain the combined effects, Langmuir sorption maxima $q_{max}$ were plotted against salinity (Fig. 5). At salinity 30‰, the $q_{max}$ of OTC reduced by 23.6% on sediment LZB and 37.4% on BHB. While at salinity 5‰, phosphate caused a decrease in the $q_{max}$ of OTC on sediment LZB by 54.3%, and on sediment BHB by 41.5%. Interestingly, the inhibition of phosphate on OTC adsorption increased with decrease of salinity. That is, phosphate had a stronger inhibitory effect on OTC adsorption at low salinity level than at high salinity level.

The above phenomenon might be explained that more phosphate anions would compete with OTC anions for adsorption sites at low salinity since phosphate adsorption increased with decreasing of salinity. We therefore hypothesized that phosphate was adsorbed preferentially. In other words, OTC had little or no impact on phosphate adsorption. This is confirmed in Fig. S2. The sorption isotherms in Fig. S2 almost
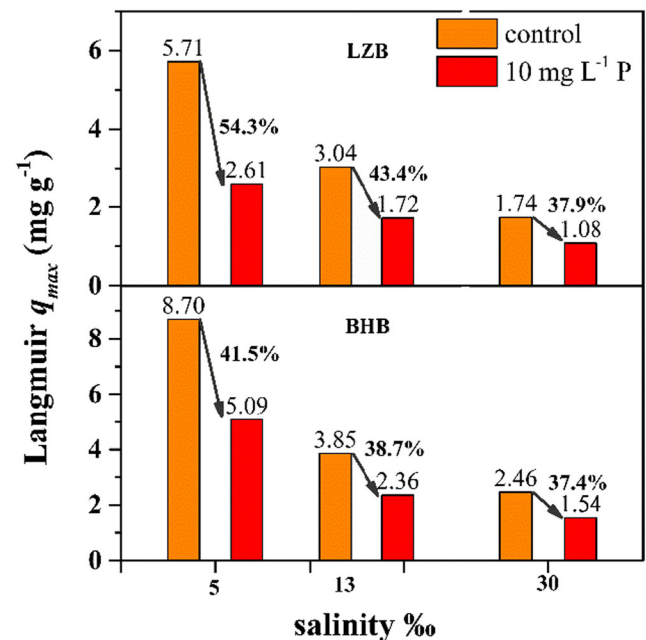


**Fig. 5** Langmuir adsorption maxima ($q_{max}$) values of OTC for sediment LZB and sediment BHB as affected by phosphate at different salinity levels

overlap and the Freundlich coefficient $K_F$ only decreased by 4.8% for sediment BHB and by 2.5% for sediment LZB after adding OTC. The inner-sphere complex formed between sediment and phosphate was obviously much stable than the non-specific adsorption of OTC onto sediment via ion exchange and electric attraction.

Figure 5 further indicates that OTC adsorption was less affected by phosphate anions in sediment BHB than in sediment LZB. This is not surprising, given that sediment BHB had much higher clay and organic carbon contents than LZB, thus a greater adsorption capacity than sediment LZB. Sediment BHB could provide more adsorption sites for these anions, which decreased the competition of phosphate with OTC for adsorption.

## FTIR analysis

The FTIR spectra of marine sediments before and after OTC adsorption are shown in Fig. 6. The peaks on FTIR spectra are linked to the functional groups of the sediments. For the virgin marine sediment samples, the band at 1631 cm$^{-1}$ is primarily due to water directly coordinated to the exchangeable anions of the sediments (Kulshrestha et al. 2004). The peak at 1439 cm$^{-1}$ could be assigned to the antisymmetric CH$_3$ deformation band. The peaks at 1026–1030 cm$^{-1}$ are possibly corresponding to the characteristic bending of Al-OH and stretching of Si-O vibrations of weathered sheet silicates (Veerasingam and Venkatachalapathy 2014). After the reaction with OTC, the band at 1631 cm$^{-1}$ shifted to lower frequency, 1624 cm$^{-1}$. This change is a good indication of the replacement of the interlayer anions with the OTC molecules. After addition of phosphate, the peak area (1624 cm$^{-1}$) decreased slightly, indicating phosphate compete with OTC for the ion-exchangeable sites. Several new peaks of LZB at 1041 cm$^{-1}$, 1072 cm$^{-1}$, and 1084 cm$^{-1}$ may be attributed to the formation of surface complexes between OTC and Al oxides. Although the content of Al oxides of BHB is higher than that of LZB (Table S1), no new peaks are observed in

BHB. This indicated that different mechanisms are responsible for OTC adsorption on different marine sediments. In the phosphate system, the appearance of the new peaks at 567 cm$^{-1}$ and 571 cm$^{-1}$, which correspond to the groups in the phosphate, suggests that phosphate has been transferred from the solution to sediment surfaces. Apart from the new peaks of phosphate, almost no differences can be observed in the spectra of OTC in phosphate system and that in the control. We therefore deduced that phosphate has similar sorption mechanisms with OTC in seawater-sediment systems and phosphate can restrain OTC adsorption through competition for the same sorption sites.

## Desorption of OTC as affected by phosphate

Generally, adsorption can be classified as strong sorption, where interactions include covalent bond, electrostatic, and surface complexation (Peterson et al. 2010), and weak sorption (e.g., van der Waals forces). The former is usually irreversible, whereas the latter is typically accompanied by a high desorption. As discussed above, phosphate can reduce OTC adsorption. Can phosphate also promote the release of adsorbed OTC? To answer this question, background solution with different phosphate concentrations (0, 10, and 50 mg L$^{-1}$) was used to conduct desorption experiments for a total of four rounds. The percentage of OTC desorption decreased successively (Fig. 7). The total percentage of OTC desorption was 68.76% (on sediment LZB) and 70.16% (on sediment BHB), indicating OTC adsorption on the sediments was weak. The addition of phosphate enhanced OTC desorption from 68.76 to 75.66% (on sediment LZB) and from 70.16 to 73.47% (on sediment BHB). This enhanced effect on OTC desorption occurred in the first two rounds of desorption. From the third round of desorption, OTC desorption percentage was slightly higher in the control than in phosphate treatments. The successive desorption would reduce the pH and make the surface of sediments more positively charged. As a result, OTC desorption became unfavorable (Sun et al. 2012).



Fig. 6 FTIR spectra of raw sediments, and sediments reacted with OTC and phosphate
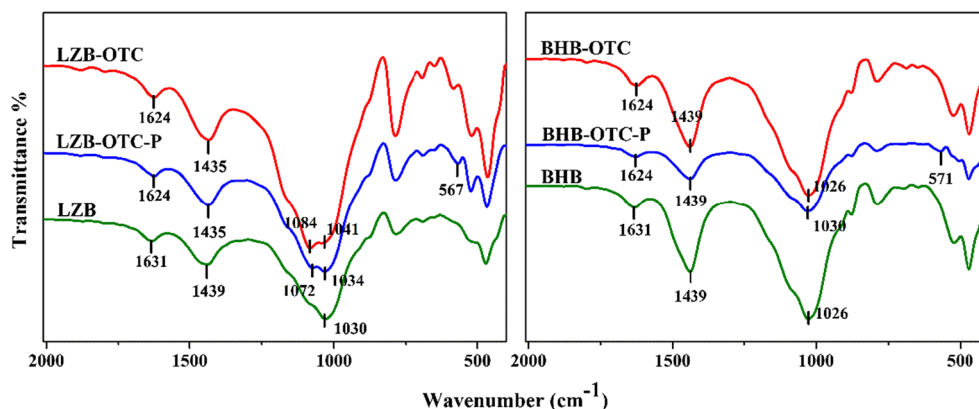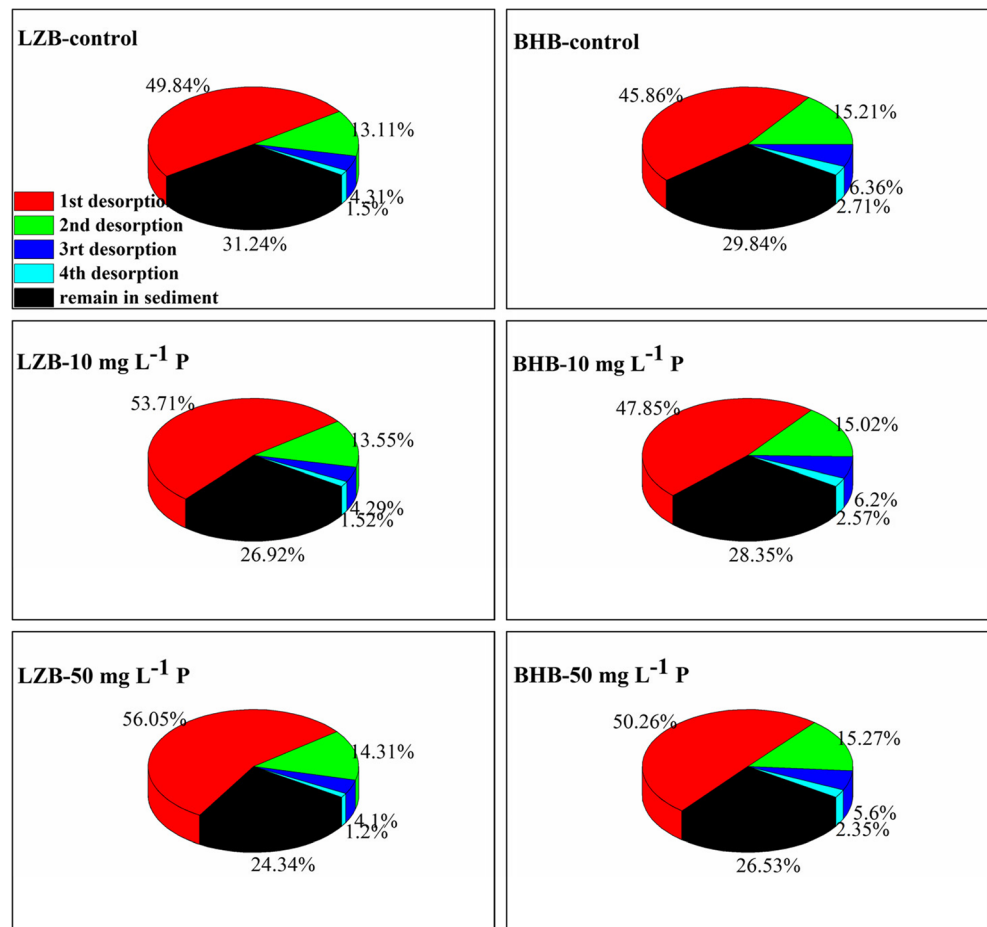
**Fig. 7** Desorption percentage of OTC as affected by phosphate with different concentrations



## Conclusions

Adsorption kinetics showed that pseudo-second-order kinetic model was more suitable to simulate the processes of OTC adsorption on marine sediments. The pseudo-second-order kinetic rate ($k_2$) of OTC increased significantly with increasing phosphate concentrations. Sediment BHB exhibited higher OTC and phosphate adsorption capacities than sediment LZB. The adsorption isotherms of OTC fitted the Freundlich and Langmuir model well. Phosphate restrained OTC adsorption, as demonstrated by the decrease of Freundlich distribution coefficients ($K_F$) and Langmuir adsorption maxima ($q_{max}$). Both phosphate and OTC adsorption decreased with increasing salinity. Phosphate showed a stronger inhibitory effect on OTC adsorption at higher salinity condition, indicating phosphate can be adsorbed preferentially. In contrast, OTC had little inhibitory effect on phosphate adsorption. FTIR analysis suggested the occurrence of ion exchange and surface complexation between OTC and sediments. Desorption experiments showed that OTC adsorption on two marine sediments were weak and phosphate could enhance the total desorption percentage of OTC. This study will provide a clue for better understanding the fate and transport of OTC in the natural coastal/estuary region.

## References

Arai Y, Sparks DL (2007) Phosphate reaction dynamics in soils and soil components: a multiscale approach. Adv Agron 94:135–179

Barbooti MM (2017) Role of organic matter, clay, and iron contents in the sorption of oxytetracycline on river sediments. Environ Eng Manag J 4:109–115

Carrasquillo AJ, Bruland GL, Mackay AA, Vasudevan D (2008) Sorption of ciprofloxacin and oxytetracycline zwitterions to soils and soil minerals: influence of compound structure. Environ Sci Technol 42:7634–7642

Figueroa RA, Mackay AA (2005) Sorption of oxytetracycline to iron oxides and iron oxide-rich soils. Environ Sci Technol 39:6664–6671

Florence AT, Attwood D (2015) Physicochemical principles of pharmacy in manufacture, formulation and clinical use, sixth edn. Pharmaceutical Press, London

Gao PP, Mao DQ, Luo Y, Wang LM, Xu BJ, Xu L (2012) Occurrence of sulfonamide and tetracycline-resistant bacteria and resistance genes in aquaculture environment. Water Res 46:2355–2364

Gao Y, Mucci A (2003) Individual and competitive adsorption of phosphate and arsenate on goethite in artificial seawater. Chem Geol 199: 91–109

Hirsch R, Ternes T, Haberer K, Kratz KL (1999) Occurrence of antibiotics in the aquatic environment. Sci Total Environ 225:109–118

Jones AD, Bruland GL, Agrawal SG, Vasudevan D (2005) Factors influencing the sorption of oxytetracycline to soils. Environ Toxicol Chem 24:761–770

Kulshrestha P, Giese RF, Aga DS (2004) Investigating the molecular interactions of oxytetracycline in clay and organic matter: insights on factors affecting its mobility in soil. Environ Sci Technol 38:4097–4105

Lebo ME (1991) Particle-bound phosphorus along an urbanized coastal-plan estuary. Mar Chem 34:225–246

Li J, Zhang H (2016) Adsorption-desorption of oxytetracycline on marine sediments: kinetics and influencing factors. Chemosphere 164:156–163

Li W, Feng X, Yan Y, Sparks DL, Phillips BL (2013) Solid-state NMR spectroscopic study of phosphate sorption mechanisms on aluminum (hydr)oxides. Environ Sci Technol 47:8308–8315

Liu HJ, Yang Y, Kang J, Fan MH, Qu JH (2012) Removal of tetracycline from water by Fe-Mn binary oxide. J Environ Sci 24:242–247

Nonaka L, Ikeno K, Suzuki S (2007) Distribution of tetracycline resistance gene, tet(M), in gram-positive and gram-negative bacteria isolated from sediment and seawater at a coastal aquaculture site in Japan. Microbes Environ 22:355–364

Peterson JW, Burkhart RS, Shaw DC, Schuiling AB, Haserodt MJ, Seymour MD (2010) Experimental determination of ampicillin adsorption to nanometer-size Al2O3 in water. Chemosphere 80:1268–1273

Song X, Liu D, Zhang G, Frigon M, Meng X, Li K (2014) Adsorption mechanisms and the effect of oxytetracycline on activated sludge. Bioresour Technol 151:428–431

Sumner DM, Belaineh G (2005) Evaporation, precipitation, and associated salinity changes at a humid, subtropical estuary. Estuaries 28:844–855

Sun Y, Yue Q, Gao B, Li Q, Huang L, Yao F, Xu X (2012) Preparation of activated carbon derived from cotton linter fibers by fused NaOH activation and its application for oxytetracycline (OTC) adsorption. J Colloid Interface Sci 368:521–527

Ter Laak TL, Gebbink WA, Tolls J (2006) The effect of pH and ionic strength on the sorption of sulfachloropyridazine, tylosin, and oxytetracycline to soil. Environ Toxicol Chem 25:904–911

Turku I, Sainio T, Paatero E (2007) Thermodynamics of tetracycline adsorption on silica. Environ Chem Lett 5:225–228

Vasudevan D, Cooper EM (2004) 2,4-D sorption in iron oxide-rich soils: role of soil phosphate and exchangeable Al. Environ Sci Technol 38:163–170

Veerasingam S, Venkatachalapathy R (2014) Estimation of carbonate concentration and characterization of marine sediments by Fourier transform infrared spectroscopy. Infrared Phys Technol 66:136–140

Wang JT, Hu J, Zhang SW (2010a) Studies on the sorption of tetracycline onto clays and marine sediment from seawater. J Colloid Interface Sci 349:578–582

Wang Q, Li Y (2010) Phosphorus adsorption and desorption behavior on sediments of different origins. J Soils Sediments 10:1159–1173

Wang YJ, Sun RJ, Xiao AY, Wang SQ, Zhou DM (2010b) Phosphate affects the adsorption of tetracycline on two soils with different characteristics. Geoderma 156:237–242

Xu RK, Xiao SC, Zhang H, Jiang J, Ji GL (2007) Adsorption of phthalic acid and salicylic acid by two variable charge soils as influenced by sulphate and phosphate. Eur J Soil Sci 58:335–342

Xu XR, Li XY (2010) Sorption and desorption of antibiotic tetracycline on marine sediments. Chemosphere 78:430–436

Zhang GS, Liu HJ, Liu RP, Qu JH (2009) Removal of phosphate from water by a Fe-Mn binary oxide adsorbent. J. Colloid Interface Sci 335:168–174

Zhang JZ, Huang XL (2011) Effect of temperature and salinity on phosphate sorption on marine sediments. Environ Sci Technol 45:6831–6837

Zhang QQ, Ying GG, Pan CG, Liu YS, Zhao JL (2015) Comprehensive evaluation of antibiotics emission and fate in the river basins of China: source analysis, multimedia modeling, and linkage to bacterial resistance. Environ Sci Technol 49:6772–6782

Zhang XX, Zhang T (2011) Occurrence, abundance, and diversity of tetracycline resistance genes in 15 sewage treatment plants across China and other global locations. Environ Sci Technol 45:2598–2604

Zwolsman JJG (1994) Seasonal variability and biogeochemistry of phosphorus in the Scheldt estuary, south-west Netherlands. Estuar Coast Shelf Sci 39:227–248